Heliyon 7 (2021) e07394

Contents lists available at ScienceDirect

Heliyon

journal homepage: www.cell.com/heliyon

Research article

Reliable determination of the growth and hydrogen production parameters of the photosynthetic bacterium *Rhodobacter capsulatus* in fed batch culture using a combination of the Gompertz function and the Luedeking-Piret model

Jonathan Deseure [a,*], Jamila Obeid [a,b], John C. Willison [c], Jean-Pierre Magnin [a]

[a] Univ. Grenoble Alpes, Univ. Savoie Mont Blanc, CNRS, Grenoble INP, LEPMI, 38000, Grenoble, France
[b] Al Baath University, Faculty of Chemical and Petroleum Engineering, Homs, Syria
[c] Laboratoire de Chimie et Biologie des Métaux (UMR 5249 CEA-CNRS-UGA), DRF/IRIG/DIESE/CBM, CEA-Grenoble, 38054, Grenoble, France

ARTICLE INFO

Keywords:
Photofermentation modeling
Hydrogen production
Rhodobacter capsulatus
Quasi-continuous fermentation

ABSTRACT

In this study, experimental results of hydrogen producing process based on anaerobic photosynthesis using the purple non-sulfur bacterium *Rhodobacter capsulatus* are scrutinized. The bacterial culture was carried out in a photo-bioreactor operated in a quasi-continuous mode, using lactate as a carbon source. The method is based on the continuous stirred tank reactors (CSTR) technique to access kinetic parameters. The dynamic evolution of hydrogen production as a function of time was accurately simulated using Luedeking-Piret model and the growth of *R. capsulatus* was computed using Gompertz model. The combination of both models was successfully applied to determine the relevant parameters (λ, μ_{max}, α and β) for two *R. capsulatus* strains studied: the wild-type strain B10 and the H_2 over-producing mutant IR3. The mathematical description indicates that the photofermentation is more promising than dark fermentation for the conversion of organic substrates into biogas.

1. Introduction

Economic development over the last few decades has been strongly dependent on fossil fuels as sources of energy. These resources are not unlimited in the long term, and environmental concerns have led to the search for clean, renewable energy sources. Urban/agro-industrial/agricultural wastes appear as relevant energetic resources in a sustainable energy mix. Biogas results from the anaerobic digestion of organic matter that, is the main constituent of these wastes. Indeed, the production of methane or hydrogen from the biomass follows the principle of the fermentation. Hydrogen is considered as the more sustainable energy carrier due to the high efficient end-use technologies such as the fuel cells [1, 2]. Clean-hydrogen gas can be produced either by electrolysis [3], steam biomethane reforming [4], biomass gasification [5], or biological synthesis [6, 7].

Biohydrogen production processes, are divided into two groups according to the dependency on light: dark and photo fermentations [8, 9]. Under dark anaerobic conditions, the organic substrates and waste waters are metabolized to form hydrogen and lower molecular weight organic acids. Photofermentative hydrogen production, issued from oxidation of organic compounds, occurs under anaerobic, nitrogen-limited conditions, utilizing light as energy source. A wide range of photosynthetic bacteria has been reported to produce hydrogen, including *Rhodobacter capsulatus*, *Rhodobacter sphaeroïdes*, *Rhodopseudomonas palustris,* and *Rhodospirillum rubrum* [10, 11]. Among them, *Rhodobacter capsulatus* is a favorable candidate for large-scale production due to its high energy and substrate conversion efficiencies and its ability to utilize a wide variety of substrates for growth and hydrogen production [12, 13].

The rate and yield of hydrogen production is greatly dependent on the carbon source used, physiological growth conditions, such as light intensity [14, 15], and bacterial growth mode. Fed-batch growth mode is recognized as the most suitable operation mode for H_2 production, in comparison with batch and continuous modes [16]. In fact, studies for H_2 production during fed-batch conditions by photosynthetic bacteria have been reported for *Rhodopseudomonas palustris* sp. and *R. palustris* 42OL (on acetate and malate as carbon source, respectively) [17, 18],

* Corresponding author.
E-mail address: jonathan.deseure@lepmi.grenoble-inp.fr (J. Deseure).

https://doi.org/10.1016/j.heliyon.2021.e07394
Received 9 January 2021; Received in revised form 29 April 2021; Accepted 21 June 2021

R. sphaeroïdes ZX-5 (on malate) [19], *R. faecalis* RLD-53 (on acetate) [20], and *R. capsulatus* DSM1710 (on acetate) [13].

Various kinetics models have been derived for biohydrogen production, as previously reviewed [21, 22]. In particular, and because of its simple initial form, the Luedeking-Piret model, developed in 1959 to describe lactic acid production and others processes [23, 24], has recently been applied to fermentative hydrogen production. In this widely used mathematical model, the rate of product formation (like hydrogen) can be related to both biomass concentration and microbial growth rate. All the studies concerned dark fermentation conditions with the exception of one devoted to the phot osynthetic bacterium, *R. palustris* [25].

Unfortunately, comparison between studies is quite complicated because the use of batch culture and different operating conditions makes it difficult to determine Luedeking-Piret model parameters from the published data. The estimation of not directly quantifiable compounds is essential in the development of biotechnology processes like photo-hydrogen production. However, a complex model involves several kinetics parameters and it is difficult to discuss the relevance of each one. It is also difficult to use traditional batch techniques, without complex model, to scrutinize useful parameters. This problem is theoretically overcome with continuous stirred tank reactors (CSTR) inside which the composition is uniform at any point. For a given mean residence time ($\frac{V}{Q}$) and inlet and outlet concentrations, the mass balance is very simple and it is hence easy to calculate the kinetic constants. In practice, the stirring of bioreactor is well achieved with a good mixing but the inlet flow rate must be adapted to avoid wash-out of microbial biomass.

The present study describes a mathematical approach to determine reliable kinetic parameters of hydrogen production by the photosynthetic bacterium, *R. capsulatus*, in a quasi-continuous photobioreactor. The developed mathematical/experimental approach is simple enough in terms of mathematical complexity and experimental procedure to be further used to attain reliable parameter values (α, β) of Luedeking-Piret model or maximum growth rate (μ_{max}) and lag time (λ). The present work combines Luedeking-Piret model and Gompertz model using the main assumptions of continuous stirred-tank reactor (CSTR) operation.

2. Material and methods

2.1. Bacteria and culture medium

Rhodobacter capsulatus strains B10 and IR3 [26] were grown anaerobically at pH 6.8 and 30 °C in modified RCV medium. The modified medium RCV, derived from [27], contained Na-lactate (35 mM), Na-Glutamate (7 mM), phosphate buffer (K_2HPO_4/KH_2PO_4, 5.17 and 4.41, mM), and a solution of salts containing different salts as oligoelements such as Mo (1.5μmol) and Fe (42 μmol).

2.2. Photo-bioreactor

Hydrogen producing experiments were carried out in a laboratory-made, rectangular-shaped 1 L bioreactor operated in the fed batch mode [28]. Anaerobic conditions were obtained by initially purging the bioreactor with sterile argon gas. Temperature and pH values were acquired by two pH and temperature probes connected to a computer via an acquisition card (Measurement Computing SA, PMD1208 LS). The pH was controlled with a pH regulator and pumps, by automatic addition of sodium hydroxide (2 M). The hydrogen flow rate was measured by a mass flow meter (Mac Millan, model 50D, 0–20 ml H_2 h^{-1}) linked to the data acquisition card. Hydrogen volume was obtained by time-integrating the hydrogen flow rate furnished by the flow-meter.

The substrate flow during fed-batch culture was controlled by a single pump functioning in both directions and electro-valves (Sirai, Type Z130A, V12). The entry flow was identical to the output flow in order to maintain a constant culture volume. The pump and electro-valves were controlled using the digital channels of the acquisition card, interfaced with a lab-made software based on Visual Studio.

The bioreactor was illuminated from one side by a sodium-vapor lamp (OSRAM, Plantastar, 600 W). The light intensity at the surface of the reactor was varied by changing the distance between the light source and the illuminated surface. The light intensity was measured with a digital lux meter (Meter, RO 1332).

The dynamics of the bacterial population and the hydrogen production were measured in quasi-continuous mode. The culture was started in batch mode, then when a constant bacterial protein concentration was reached *ca.* 0.45 g/l for B10 and *ca.* 0,36 g/l for IR3. As soon as the bacterial concentration was reached, the quasi-continuous conditions were applied. During continuous operation, the culture was fed with RCV growth medium containing 35.7 mM (4 g/L) sodium lactate and 5 mm sodium glutamate at a rate of 1 ml min^{-1} and bacterial culture was withdrawn at the same rate over a 30–50 h period. The withdrawal and feeding were then interrupted and the culture operated in batch mode for 6 h. These quasi -continuous conditions were repeated 3–5 times period of 100–200 h for both *R. capsulatus* strains. In the case of strain IR3, the final batch mode was prolonged until stationary phase was achieved.

2.3. Analytical methods

Samples were regularly withdrawn for determining the concentrations of biomass and substrate. The bacterial cell concentration was estimated by measuring the optical density at 660 nm according the relation OD 0.8 corresponded to 0.37 mg dry weight L^{-1} and 0.16 mg protein L^{-1}. Lactate concentration was measured by HPLC (Agilent 1260, column Hi Plex H 8μm) using a Refractive Index Detector G1362A – Agilent. Sample was firstly centrifuged (16,060 g, 5 min) and the supernatant was diluted 10 times and finally filtered (0.2 μm porosity) before analysis. The mobile phase for HPLC was a solution of sulfuric acid 2.3 mM (0.4 ml min^{-1}). Calibration curves were generated using standards of ultrapure lactic acid.

2.4. Mathematical approach

The Gompertz function, available since 1825, can be used as exponential model to take into account the slowing down of the observed growth of the batch reactor culture of any microorganism. The Gompertz function can describe the dynamics of any living form without limitation of resources. Consequently, the Gompertz function [29] is well adapted to biological reactors with efficient substrate renewal.

The Gompertz equation is given by:

$$ln\left(\frac{X}{X_0}\right) = ae^{-e^{(b-ct)}} \tag{1}$$

We call this relationship $f(t)$ and the associated equation is

$$g(t) = X_0 e^{ae^{-e^{(b-ct)}}} \tag{2}$$

where X is the bacterial density or protein concentration and X_0 is the initial bacterial density or initial protein concentration. First and second derivatives of $f(t)$ are given by the equation (3) and equation (4):

$$f'(t) = ace^{(b-ct)-e^{(b-ct)}} \tag{3}$$

$$f''(t) = ac^2 e^{(b-ct)-e^{(b-ct)}}\left(e^{(b-ct)} - 1\right) \tag{4}$$

Gibson *et al.* [29] have coupled logistic models and the Gompertz function; however the Gompertz function is not directly interpretable. To solve this problem, Zwietering *et al.* [30] simplified the two models by incorporating the classic parameters of maximum concentration, latency time and maximum growth rate. However, it is also possible to determine these parameters using the nonphysical parameters (raw parameters) of

the Gompertz function (a, b, c) using the undermentioned equations. The time of inflexion point is the solution of the following equation:

$$f''(t_i) = 0 \tag{5}$$

Which involves:

$$t_i = \frac{b}{c} \tag{6}$$

And the maximum growth (μ_{max}) rate is given by:

$$\mu_{max} = f'(t_i) \tag{7}$$

The lag time (λ) is the intercept with x-axis of the tangent line:

$$f'(t_i)t + y_{(t=0)} = 0 \tag{8}$$

And the maximum concentration is the asymptote of Gompertz function:

$$\overline{X} = \lim_{t\to\infty} X_0 e^{ae^{-e^{(b-ct)}}} = X_0 e^a \tag{9}$$

Overall techniques are well known, but few experimental cultures correspond to the simple sigmoid function (Gompertz function). In other hand, Luedeking-Piret model can well describes the fermentative process; this classical model considers the relationship of cell growth to product formation as follow:

$$\frac{dP}{dt} = \alpha\frac{dX}{dt} + \beta X \tag{10}$$

In the present study, we have coupled the Luedeking-Piret model and the Gompertz function. However, some assumptions were required to this combine:

- there is no limitation by the substrate [20].
- the decrease in bacterial density (wash-out of microorganisms during the continuous process (CSTR technic only) affects weakly the Gompertz description (asymptote value only).

All the assumption are validated by as smooth quasi-continuous feed [31] and the simple automation such as presented above. These assumptions are validated in the section 3.1. Therefore the Eq. (1) and their derivative expression, as follow:

$$\frac{dP}{dt} = \alpha f'(t)g(t) + \beta g(t) \tag{11}$$

And the integration of this equation is given by:

$$P(t) = \alpha X_0\left(e^{ae^{-e^{(b-ct)}}}\right) + \beta X_0 \int_0^t e^{ae^{-e^{(b-cx)}}}\,dx \tag{12}$$

In addition, it is possible analyze the mathematical function (12) and to observe for the time tr ≅ 3. ti (where more of 95% of maximum concentration (asymptote of Gompertz function) is obtained) that the dynamic hydrogen production could be described by a linear evolution for t >> tr as follow:

$$P(t) \cong \beta\overline{X}t \tag{13}$$

3. Results and discussion

3.1. Experimental measurements of bacterial growth and substrate consumption

Kinetics of bacterial production and substrate consumption for the wild type *R. capsulatus* B10 and the H_2 over-producing strain IR3 were shown in Figures 1A-1B, respectively.

For the wild type B10 strain, the first feeding procedure started at the beginning of the batch stationary phase (Figure 1A), when lactate was almost completely metabolized (concentration close to 0 g $L^{-1)}$. The application of continuous flow conditions led to an increase in lactate concentration to 0.7 g L^{-1}, concomitant with a decrease in bacterial protein concentration from 0.54 to 0.44 g L^{-1}. Interruption of continuous flow followed by batch culture then led to a stabilization at 0.7–0.8 g lactate L^{-1} and 0.44–0.48 g protein L^{-1}. This was repeated over 3 cycles of quasi-continuous operation.

For the H_2 over-producing strain IR3, the feeding procedure started at the end of the exponential growth phase, after the consumption of 90% of lactate (residual concentration of 0.4 g L^{-1}). The feeding of growth medium led to an increase in lactate concentration to 1 g L^{-1} and a decrease in bacterial protein concentration from 0.4 g L^{-1} to 0.35 g L^{-1}. Alternation of continuous and batch modes led to a stabilization at 0.34–0.38 g protein L^{-1} and 0.75–0.95 g lactate L^{-1}, and this was repeated over 5 cycles of quasi-continuous operation. The final, prolonged batch phase led to complete consumption of lactate and a final bacterial concentration of 0.45 g L^{-1}.

In both case the decrease in bacterial concentration due to wash-out during the continuous mode operation was computed to be close to 20 mg of proteins per hour for an average flow rate < 1 ml min^{-1}. This is small compared to the potential range of biomass production in the reactor of 100–350 mg protein per hour. Taken together with the lack of substrate limitation (stabilization at 0.7–0.95 g lactate L^{-1}), these results validate the assumptions of the Gompertz model.

3.2. Fitting procedure and parametric values

The aim of the "data fitting" is to determine and compare parameter values of the model that describes the process. On the other hand, the parametric optimization is also a useful tool for validating the model.

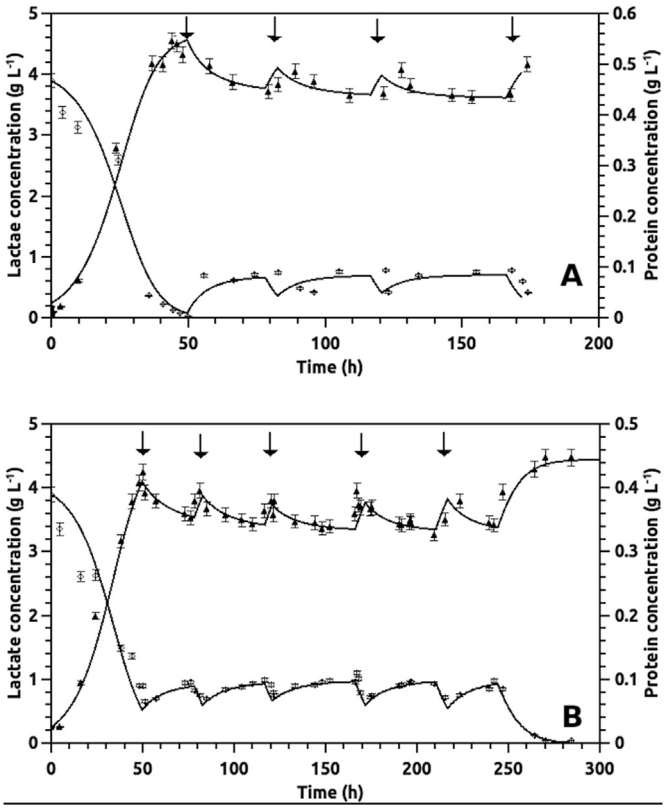

Figure 1. Kinetics of the lactate consumption (S, ◊) and the bacterial production (X, ▲) during a quasi-continuous culture of *R. capsulatus* B10 (A) and IR3 (B). the arrows indicate the application of continuous flow.

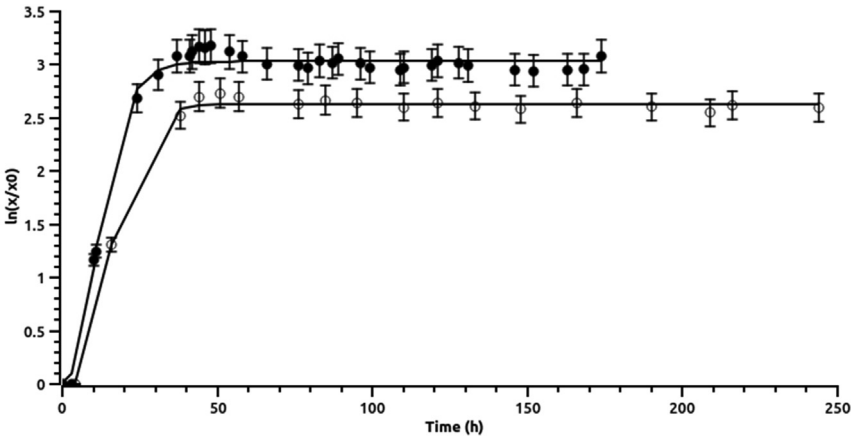

Figure 2. Bacterial growths in quasi-continuous culture of wild strain B10 (●) and over-producer strain IR3 (○): experimental data and Gompertz simulation.

Nevertheless, the fitting procedure requires an appropriate attention to achieve relevant results. The Gradient methods are generally more efficient when the objective function is continuous in its first derivative. Gradient methods use information about the slope of the function to dictate a direction of search where the minimum is thought to lie. The simplest of these is the method of steepest descent in which a search is performed in an opposite direction of gradient of the objective function. This method is available with numerous commercial software. Gompertz function and (Eq. 1) coupled Luedeking-Piret model and Gompertz function (Eq. 12) are expedient mathematical functions to achieve the conventional numerical optimizations.

Bacterial growth was modeled using the Gompertz function; and Figure 2 shows good agreement between the model and experimental values of biomass concentration. Table 1 compares the a, b and c values for the *R. capsulatus* strains. However, no direct interpretation is possible as these are raw parameters, and the Eqs. (5), (6), (7), and (8) must be used in order to obtain meaningful physical parameters, such as μ_{max}, λ, and Y_{xS}.

In this context, λ is the intercept with x-axis of the tangent line as expressed in the Eq. (7), μ_{max} is given by the derivative function of Gompertz model (Eq. (7)) and Y_{xS} is directly obtained from Eq. (9) and the initial substrate concentration.

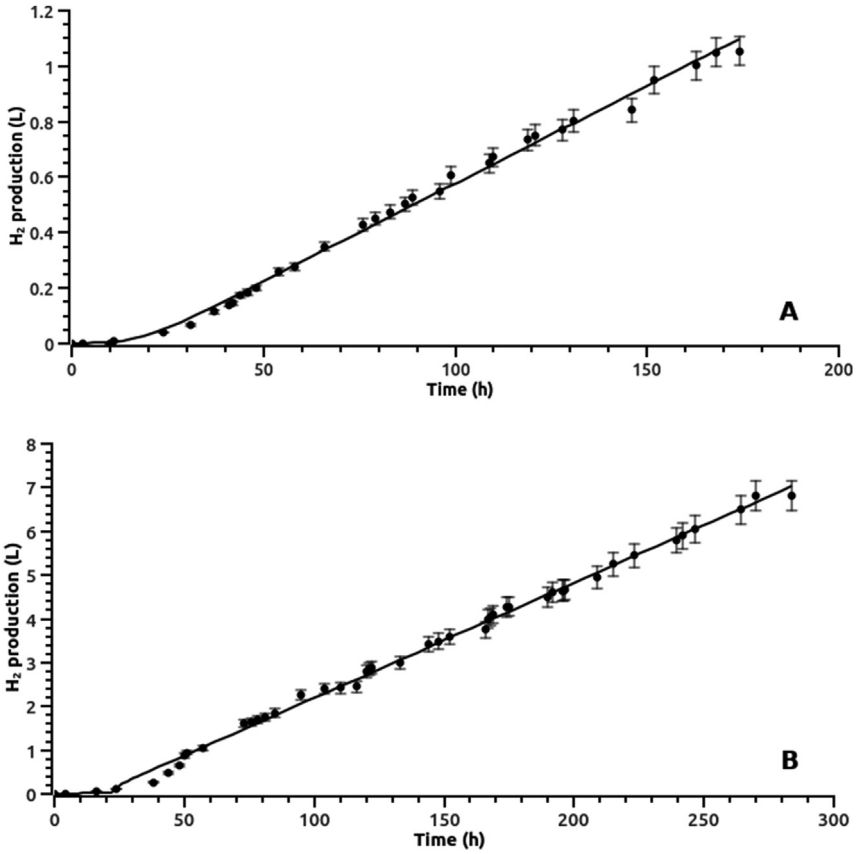

Figure 3. Simulated Luedeking–Piret's model coupled Gompertz equation to and H_2-production by *Rhodobacter capsulatus* B10 (A) and IR3 (B) (35 mM lactate, 30,000 Lx).

Table 1. Gompertz function parameters.

	B10	IR3
a [-]	3.03	2.66
b [-]	1.77	2.18
c [h^{-1}]	0.174	0.1581
R^2	0,9924	0.9968

The growth-associated product coefficient, α, and the non-growth-associated product coefficient, β, were the determined by numerical optimization from experimental data and the Luedeking-Piret model Eq. (12) (i.e. data fitting). Experimental data for H_2 production were correctly modelled for both strains B10 and IR3, as shown in Figure 3, and the fitted parameters are summarized in Table 2.

The corresponding physical parameters, μ_{max}, Y_{xS}, λ, α, β were summarized in Table 2.

μ_{max} and λ parameters differed according to the basic growth observation of both bacterial strains. The value of the maximum specific growth rate, μ_{max}, was higher for the wild type strain B10 (0.195 h^{-1}) than the one observed for the over-producer strain IR3 (0.166 h^{-1}). In addition, the wild strain B10 grew earlier than the mutant strain IR3 with a similar substrate utilization rate, Y_{XS}: 0.124 and 0.109 g protein g^{-1} lactate, respectively B10 and IR3, this was correlated with a lower lag time observed for the wild type B10 (9.8 h) compared to the mutant IR3 (13.9 h).

The Luedeking-Piret model implies that hydrogen production is associated with both non-growth and growth-associated terms. The growth-associated term indicates that hydrogen production (α) is proportional to the bacterial growth rate. On the other hand, the non-growth associated term (β) signifies that hydrogen production is linearly dependent on biomass concentration. In the case of strain IR3, both parameters were substantially higher than for the wild type strain B10 (see Table 2). It is noteworthy that the β parameter is main parameter to describe hydrogen production by photofermentation. Eq. (13) shows that it possible to model fermentation products using a linear relationship, assuming a negligible artificial mortality and biomass dilution during the continuous or quasi-continuous process:

$$P(t) = b + \beta \overline{Xt} \quad (14)$$

Therefore, the non-growth associated term could be attained by direct linear regression and the parameters determined by the linear procedure (equation 13) were very close to those obtained by the overall simulation of the Luedeking–Piret model. Both mathematical procedures can provide realistic β parameters, which is the most important parameter when selecting a productive strain. One cannot estimate α separately using batch culture data (Eq. (12)), except for t << tr, and concomitant α and β fitting is complicated by the necessary approximations of growth. Thus, in the case of batch cultures, realistic estimations of β and α require much additional data.

Table 2. Fitted parameters of Luedeking–Piret's model and associated growth parameters.

	B10	IR3
Y_{XS}	0.124	0.109
λ [h]	9.8	13.9
μ_{max} [h^{-1}]	0.195	0.166
β [ml H_2 (g L^{-1})$^{-1}$ h^{-1}]	17	72
α (ml (g L^{-1})$^{-1}$)	4.5	36.6
R^2	0.9980	0.9975
β [ml H_2 (g L^{-1})$^{-1}$ h^{-1}] (linear regression)	14	75.6
R^2	0.9942	0. 9969

3.3. Discussion

Using the Gompertz function to model bacterial growth and the Luedeking-Piret model to describe hydrogen production by *R. capsulatus* during quasi-continuous culture, good agreement was observed between the experimental data and the models, with high regression coefficient values (R^2) exceeding 0.99 in all cases (Table 2). The β and α parameters were lower in the wild type strain B10 than in the H_2 over-producer mutant IR3, as previously observed in batch culture [28]. The authors showed that the specific hydrogen production rate (ml h^{-1}) is proportional to the light intensity, which is the multiplying factor applied to non-growth -associated term (β) of Luedeking-Piret model. As above, in the present study, the wild type B10 exhibited a maximum specific growth rate, μ_{max}, higher (0.195 h^{-1}) that the over-producer strain IR3 (0.166 h^{-1}), this latter converted more efficiently the substrate (lactate) in product (H_2) that the wild-type B10 strain.

The maximum growth rate observed in indoor culture on synthetic medium with the wild-type *R. capsulatus* B10, on lactate-glutamate (35/5 mM as carbon and nitrogen source, is comparable with this obtained with the strain 37b4 on malate-$(NH_4)_2SO_4$ (16/9.5 mM), 0.195 and 0.251 h^{-1} [32]. However, much lower maximum growth rates were observed in outdoor fed batch cultures on acetate-glutamate medium of *R. capsulatus* DSM1710 and the hydrogenase-deficient mutant YO3 (0.025 h^{-1} and 0.052 h^{-1}, respectively [13, 33]. By contrast, in the present study both strains (IR3 and B10) exhibit similar values of the conversion rate of

Table 3. H_2-producing processes described by the original or modified forms of the Luedeking-Piret (LP) model.

Biomass	α value (ml g^{-1} VSS[a])	β value (ml H_2 g^{-1} dw h^{-1})	Reactor type	substrate	Fermentation/LP model	Ref.
R. palustris	6.85[b]	0.41[b]	batch	glycerol	Light/modified	[25]
R. capsulatus						
B10	4.5[c]	17[c]	Quasi-continuous	Lactate	Light/modified	This study
IR3	36.6[c]	72[c]				
Mangrove sediments	11.04	0	batch	glucose	Dark/original	[35]
Local sewage sludge	224	0	continuous	sucrose	Dark/[e] $r_{H2} = D\alpha X$	[36]
Anaerobic sludge	759	0	batch	glucose	Dark/original	[37]
Anaerobic sludge	793	0	batch	glucose	Dark/original	[38]
Enterobacter cloacae	166[d]	0	batch	glucose	Dark/original	[39]
Clostridium pasteuranium	918	0	batch	xylose	Dark/dP/dt = α(1/X.dX/dt)	[40]
	876	0		sucrose		

[a] Volatile Suspended Solids.
[b] undefined.
[c] $\alpha = 1/Y_{XP}$ expressed in ml H_2 g protein L^{-1} and β in ml H_2 (g L^{-1})$^{-1}h^{-1}$.
[d] ml H_2 g^{-1} cell mass.
[e] D = liquid phase dilution rate, X = biomass concentration.

Table 4. H_2-producing processes based on fed-batch regime. These processes have been previously summarized by Argun and Kargi 20], Androga *et al.* [41], Sagnak and Kargi [42], Basak *et al.* [16], and Uyar et al. [43].

Strains	Carbon and nitrogen sources	Photobioreactor characteristics and operating conditions	Fed batch, semi continuous conditions	Maximal H_2 productivity[a] ($mM\ H_2\ L^{-1}$ medium h^{-1})	Substrate conversion efficiency (mol H_2 mol^{-1} carbon source)	Ref.
R. sphaeroïdes B6 (thermostable)	Lactate (25 mM) Na Glutamate (5 mM)	6-L plate polyacrylate outdoor	15 % dilution/4 days	1.07–1.56 (fine weather) 0.61–1 (cloudy weather) 0.09–0.56 (rainy weather)	3.51[a]	[44]
Rhodopseudomonas capsulata	Glucose DFE[b]: acetate (8.5 mM) propionate (1.7 mM) butyrate (13.6 mM) Na Glutamate (3 mM)	1.5-L indoor	HRT[c]: 72 h	0.65	1.6 (acetate) 2.8 (propionate) 4 (butyrate)	[45]
	acetate (30.5 mM) propionate (2 mM) butyrate (9 mM) Na Glutamate (3 mM)	1.5-L indoor	HRT[c]: 72 h	0.8	ND	
	acetate (11.5 mM) propionate (3 mM) Na Glutamate (3 mM)	1.5-L indoor	HRT[c]: 72 h	0.94	ND	
Rhodopseudomonas palustris 42OL	Malic acid (24.3 mM) Glutamic acid (5.6 mM)	1.07 L cylindric glass pH 6.8 320 W m^2 408-h duration	ND small concentrated stock solution volume replacing sampling volume	0.49	ND	[46]
Rhodopseudomonas palustris sp.	Acetate (66.7 mM) Glutamic acid (5.6 mM)	Cylindric glass (0.22 L) pH 6.8–7.2 4 W m^2 indoor	10% withdraw (experimental condition SC[d] 240h)	0.39	1.6	[17]
Clostridium acetobutylicum DSM792 + R. sphaeroïdes O.U.O O 1	Non pretreated wheat starch from corn (C source)/yeast extract (0.5)[e] and peptone (1)[e]	cylindrical reactor (0.25 L/0.12 L)[f] controlled pH 7 192 W/m^2 Light/Dark ratio[g] = 2	OLR[h] 1.5 g starch L^{-1} d^{-1} 2.5 % volume of medium replaced every day 0.375 g OLR L^{-1} d^{-1}	1.03	2.62 (average on 33 days)	[47]
Clostridium butirycum N1VLB-B-3060 + R. sphaeroïdes VKM-3050	Starch (4.5)[c]/yeast extract (0.04)[c], Na Glutamate (0.9)[c]	Hungate tube (16 ml/8 ml)[d] Microaerobic conditions pH7.5 30 W/m^2 Light/Dark ratio[g] = 2.28	95–96 % volume of medium replaced	ND	5.2	[48]

[a] calculated from data.
[b] Dark Fermentation Effluent.
[c] Hydraulic Retention Time.
[d] Semi continuous, culture volume withdraw.
[e] expressed in g L^{-1}.
[f] working volume/total volume of reactor.
[g] Light fermentative biomass/Dark fermentative biomass concentration ratio.
[h] Organic Loading Rates.

product/biomass. Hydrogen yields can be expressed according to different form like g or L hydrogen per g^{-1} biomass, or by lactate conversion rate. The latter was based on the theoretical total conversion (100%) of 1 mol of lactate leading to the formation of 6 mol of hydrogen. For both strains, the first step of culture corresponding to batch conditions led to a weak lactate conversion, 4.5 and 18.6 % of lactate conversion for B10 and IR3, respectively. During the quasi-continuous process, B10 strain exhibited a weak lactate conversion rate compared to the over-producer strain IR3, 26.7 % and 95 %, respectively. These values were equivalent to 0.36 and 1.1 L H_2 g^{-1} lactate, representing 27 mg and 110 mg H_2 g^{-1} lactate, for B10 and IR3 strains, respectively.

It is essential to point out the assessments of Luedeking-Piret parameters in the literature in order to understand the values obtained in this study. Table 3 summarizes the H_2 production processes, based either on dark or light fermentation, and modeled by the Luedeking-Piret model. The modeling of dark fermentation processes only implied the hydrogen production associated to the biomass growth; β value was equal to zero. At the opposite, the H_2-producing process based on photosynthetic biomass involved both a non-growth and a growth-associated hydrogen production. Our results are the first study devoted to the robust estimation of λ, μ_{max}, α and β parameter. It shows that β parameter is main parameter to describe kinetic of gas production by photofermentation, therefore dark anaerobic conditions present lower potential of volatile fatty acid conversion into hydrogen than light anaerobic conditions. In addition, the production rates of hydrogen by *R. capsulatus* with respect to light intensity irrespective of cell concentration have been previously described by Obeid *et al* [28] and Androga *et al* [34]. Authors showed that the specific hydrogen production rate (ml h^{-1}) is proportional to the light intensity, which is the multiplying factor applied to non-growth -associated term (β) of Luedeking-Piret model.

Since the first study [44] devoted to the outdoor H_2 production during a fed-batch culture of *Rhodopseudomonas sphaeroïdes,* many studies with PNS (purple-non-sulfur) bacteria have been carried out in different culture modes including fed-batch, repeated conditions or semi and continuous condition. They were summarized by Argun and Kargi [20], Androga et al. [41], Sagnak and Kargi [42], Basak *et al.* [10], and Uyar *et al.* [43]. Table 4 incorporates these and more recent data based on fed-batch and semi-continuous H_2 production processes using either pure PNS cultures or co-cultures with dark fermentative bacteria. Indoor conditions represented the majority of previous fed-batch studies, using different light source and intensity as tungsten, halogen, fluorescent, incandescent, and Na vapor light. Nature and use of different unities of

Table 5. Comparison of the H_2 productivity and substrate conversion ratio obtained by *Rhodobacter capsulatus* strains under fed-batch, continuous and semi-continuous conditions.

Carbon sources	Photo-bioreactor	Growth mode	Location	Studied biomasses	Maximal H_2 productivity (mL H_2 L^{-1} medium h^{-1})	Substrate conversion efficiency (mol H_2 mol^{-1} carbon source)	Ref.
Lactate (35 mM) Na Glutamate (5 mM)	1-L PMMA panel	semi-continuous	Indoor	B10, wild-type	0.26	0.24	This study
				IR3, H_2 over producer	0.41	0.75	This study
Acetate (40 mM) Na Glutamate (2 mM)	4L–8L PMMA panel	fed-batch (10 L daily feeding)	outdoor	YO3, hup$^-$ mutant	0.51	0.53	[51]
	80-L PMMA tubular	fed-batch (10 L daily feeding)	outdoor	DSM1710, wildt type	0.31	0.60	[32]
				YO3, hup$^-$ mutant	0.40	0.35	[13]
Lactate (4 mM) Acetate (23 mM) Na Glutamate (1.37 mM)	65-L PMMA panel	continuous (daily replacement of 20 % volume reactor)	outdoor	DSM155, wild-type	0.36	ND	[52]
	4 * 25-L PMMA tubular	continuous (daily replacement of 20 % volume reactor)	outdoor	DSM155, wild-type	0.15	ND	[16]
Sugar beet thick juice DFE[a] (Acetate 42 mM, NH_4^+ 2.2 mM, Total nitrogen 3.3 mM)[b]	4-L PMMA panel	fed-batch (10% daily feeding v:v)	outdoor	YO3, hup$^-$ mutant	1.12	0.77	[49]
Sugar beet thick juice DFE[a] (Acetate 31 mM, NH_4^+ 2 mM, Total nitrogen 7 mM)[c]	4-L PMMA panel	continuous (daily replacement of 10% v:v)	indoor	YO3, hup$^-$ mutant	1.01	0.48	[43]
	4-L PMMA panel	continuous (daily replacement of 10% v:v)	indoor	DSM1710, wild type	1.05	0.46	
Molasse DFE[a] (Acetate 32.5 mM, lactate 2.5 mM, Formiate 2.5 mM)[b]	4-L PMMA panel	fed-batch (10% daily feeding v:v)	outdoor	DSM1710, wildt type	0.5	0.5	[50]
				YO3, hup$^-$ mutant	0.67	0.78	

[a] Dark fermentation effluent.
[b] Supplemented with Fe-citrate and Na2MoO4,2H20, 0.1 mM and 0.16 μm, respectively.
[c] Supplemented with Fe-citrate 0.1 mM.

illumination increased the difficulty to compare experimental conditions. Recently many outdoor operating system for H_2 production by *R. capsulatus* were carried out according to reactor design, effluent nature, bacterial strains, and feeding strategy conditions (Table 5), principally with *Rhodobacter capsulatus*.

Efficiency of H_2 producing bioprocess based on PNS was habitually characterized by two principal parameters: the H2 productivity expressed as mM H2 produced L-1. h-1 and the substrate conversion ratio, which is the experimental H_2 yield divided by theoretical yield. H_2 productivity and substrate conversion ratio depend on experimental conditions as substrate nature, illumination, bacterial strain and feeding strategy conditions as indicated in previous summary tables extracted from recent reviews. In order to make the comparison more concise only results with *Rhodobacter capsulatus* strains were reported here. The production of H_2 by PNS totally depends on the enzymatic activity of nitrogenase. However, H_2 can be consumed by another enzymatic system known as uptake hydrogenase (hup). The productivity values for the wild type strain B10 and the over-producer strain IR3, extracted from Figure 3; were 0.26 and 0.41 mM H2 L-1 culture h-1, respectively. Substrate conversion ratio was calculated from oxidized lactate during semi-continuous of wild-type B10 and H_2 over-producer strain IR3. H_2 productivity value of wild-type B10 was 0.24 M M^{-1} lactate. This value was close to that of DSM155 (0.15–0.36 M M^{-1} carbon source), but lower that those obtained for the wild-type DSM1710 (0.5–0.78 M M^{-1} carbon source); irrespective to experimental conditions (Table 5). The H_2 over-producer mutant IR3 exhibited a substrate conversion ratio of 0.75. This latter was larger than the wild-type B10, but close to the maximum H_2 substrate conversion ratio obtained during fed-batch culture of the *hup-R. capsulatus mutant* YO3 on dark fermented effluents of sugar beet thick huice [49] or molasse [50] (Table 5). Therefore, our methodology provides a robust estimation of λ, μ_{max}, α and β parameter in agreement with literature results (i.e. substrate conversion ratio and H_2 productivity) which achieved under fed-batch, continuous and semi-continuous conditions.

4. Conclusions

The Luedeking-Piret model was used in this study to describe the bacterial growth, substrate consumption, and hydrogen gas production by using the purple non-sulfur bacterium *Rhodobacter capsulatus*. Hydrogen production by *R. capsulatus* during a quasi-continuous culture over a 150–200 h period was successfully controlled with various key parameters as inlet flow rate, feed volume, and dilution rate of substrate supply. The *R. capsulatus* over-producing strain IR3 displayed a greater hydrogen production yield correlated to the non-growth associated term (β). A good agreement was obtained between the experiments and simulations with high regression coefficient values ($R^2 > 0.99$). Fitting procedure allows to relevant parameters such as the lag time (λ), the maximum growth rate μmax and both non-growth (β) and growth-associated terms (α) of Luedeking-Piret model. This parameter access will be useful for comparison between strains or/and literature data and for the automation and control of bioprocesses for the continuous fermentation process.

Declarations

Author contribution statement

Jonathan Deseure, Jean-Pierre Magnin: Analyzed and interpreted the data; Contributed reagents, materials, analysis tools or data; Wrote the paper.

Jamila Obeid: Conceived and designed the experiments; Performed the experiments.

John C. Willison: Analyzed and interpreted the data; Wrote the paper.

Funding statement

Jamila Obeid was supported by the Institute of International Education's Scholar Rescue Fund, USA and the University Grenoble Alpes, LEPMI, France.

Data availability statement

Data will be made available on request.

Declaration of interests statement

The authors declare no conflict of interest.

Additional information

No additional information is available for this paper.

References

[1] L. Barreto, A. Makihira, K. Riahi, The hydrogen economy in the 21st century: a sustainable development scenario, Int. J. Hydrogen Energy 28 (2003) 267–284.
[2] T. da Silva Veras, T.S. Mozer, D. da Costa Rubim Messeder dos Santos, A. da Silva César, Hydrogen: trends, production and characterization of the main process worldwide, Int. J. Hydrogen Energy 42 (2017) 2018–2033.
[3] I. Dincer, C. Acar, Innovation in hydrogen production, Int. J. Hydrogen Energy 42 (2017) 14843–14864.
[4] R.D. Cortright, R.R. Davda, J.A. Dumesic, Hydrogen from catalytic reforming of biomass-derived hydrocarbons in liquid water, Nature 418 (2002) 964–967.
[5] P. Parthasarathy, K.S. Narayanan, Hydrogen Production from steam gasification of biomass: influence of process parameters on hydrogen yield, A Rev. Renew. Energy 66 (2014) 570–579.
[6] C.N. Dasgupta, J.J. Gilbert, P. Lindblad, T. Heidorn, S.A. Borgvang, K. Skjanes, D. Das, Recent trends on the development of photobiological processes and photobioreactors for the improvement of hydrogen production, Int. J. Hydrogen Energy 35 (2010) 10218–10238.
[7] E. Eroglu, A. Melis, Photobiological hydrogen production: recent advances and state of the art, Biores. Technol. 102 (2011) 8403–8413.
[8] K. Show, D. Lee, J. Chang, Bioreactor and process design for biohydrogen production, Biores. Technol. 102 (2011) 8524–8533.
[9] P.K. Rai, S.P. Singh, Integrated dark- and photo-fermentation: recent advances and provisions for improvement, Int. J. Hydrogen Energy 41 (2016) 19957–19971.
[10] N. Basak, A.K. Jana, D. Das, D. Saikia, Photofermentative molecular biohydrogen production by purple-non-sulfur (PNS) bacteria in various modes: the present progress and future perspective, Int. J. Hydrogen Energy 39 (2014) 6853–6871.
[11] Q. Sun, W. Xiao, D. Xi, J. Shi, X. Yan, Z. Zhou, Statistical optimization of biohydrogen production from sucrose by a co-culture of Clostridium acidisoli and Rhodobacter sphaeroides, Int. J. Hydrogen Energy 35 (2010) 4076–4084.
[12] P.C. Hallenbeck, Y. Liu, Recent advances in hydrogen production by photosynthetic bacteria, Int. J. Hydrogen Energy 41 (2016) 4446–4454.
[13] E. Boran, E. Özgür, J. van der Burg, M. Yücel, U. Gündüz, I. Eroglu, Biological hydrogen production by Rhodobacter capsulatus in solar tubular photo bioreactor, J. Clean. Prod. 18 (2010) S29–S35.
[14] T. Katsuda, T. Arimoto, K. Igarashi, et al., Light intensity distribution in the externally illuminated cylindrical photobioreactor and its application to hydrogen production by Rhodobacter capsulatus, J. Biochem. Eng. 5 (2000) 157–164.
[15] J. Meyer, B.C. Kelley, P.M. Vignais, Effect of light on nitrogenase function and synthesis in Rhodopseudomonas capsulata, J. Bacteriol. 136 (1978) 201–208.
[16] H. Argun, F. Kargi, Bio-hydrogen production by different operational modes of dark and photo-fermentation: an overview, Int. J. Hydrogen Energy 36 (2011) 7443–7459.
[17] G. Padovani, S. Vaičiulytė, P. Carlozzi, BioH2 photoproduction by means of Rhodopseudomonas palustris sp. cultured in a lab-scale photobioreactor operated in batch, fed-batch and semi-continuous modes, Fuel 166 (2016) 203–210.
[18] P. Carlozzi, M. Lambardi, Fed-batch operation for bio-H2 production by Rhodopseudomonas palustris (strain 42OL), Renew. Energy 34 (2009) 2577–2584.
[19] X. Li, Z.-Z. Dai, Y.-H. Wang, S.-L. Zhang, Enhancement of phototrophic hydrogen production by Rhodobacter sphaeroides ZX-5 using fed-batch operation based on ORP level, Int. J. Hydrogen Energy 36 (2011) 12794–12802.
[20] N.-Q. Ren, B.-F. Liu, G.-X. Zheng, D.-F. Xing, X. Zhao, W.-Q. Guo, et al., Strategy for enhancing photo-hydrogen production yield by repeated fed-batch cultures, Int. J. Hydrogen Energy 34 (2009) 7579–7584.
[21] J. Wang, W. Wan, Kinetic models for fermentative hydrogen production: a review, Int. J. Hydrogen Energy 34 (2009) 3313–3323.
[22] K. Nath, D. Das, Modeling and optimization of fermentative hydrogen production, Biores. Technol. 102 (2011) 8569–8581.
[23] R. Luedeking, E.L. Piret, A kinetic study of the lactic acid fermentation. Batch process at controlled pH, Biotechnol. Bioeng. 1 (1959) 393–412.
[24] S. Nunez, F. Garelli, H. De Battista, Product-based sliding mode observer for biomass and growth rate estimation in Luedeking–Piret like processes, Chem. Eng. Res. Des. 105 (2016) 24–30.
[25] D. Zhang, N. Xiao, K.T. Mahbubani, E.A. del Rio-Chanona, N.K.H. Slater, V.S. Vassiliadis, Bioprocess modelling of biohydrogen production by Rhodopseudomonas palustris: model development and effects of operating conditions on hydrogen yield and glycerol conversion efficiency, Chem. Eng. Sci. 130 (2015), 68–68.
[26] J.C. Willison, D. Madern, P.M. Vignais, Increased photoproduction of hydrogen by non-autotrophic mutants of Rhodopseudomonas capsulata, J. Biochem. 219 (1984) 593–600.
[27] P.F. Weaver, J.D. Wall, H. Gest, Characterization of Rhodopseudomonas capsulata, Arch. Microbiol. 105 (1975) 207–216.
[28] J. Obeid, J.P. Magnin, J.M. Flaus, O. Adrot, J.C. Willison, R. Zlatev, Modelling of hydrogen production in batch cultures of the photosynthetic bacterium Rhodobacter capsulatus, Int. J. Hydrogen Energy 34 (2009) 180–185.
[29] Angela M. Gibson, N. Bratchell, T.A. Roberts, Predicting microbial growth: growth responses of Salmonellae in a laboratory medium as affected by pH, sodium chloride and storage temperature, Int. J. Food Microbiol. 6 (1988) 155–178.
[30] M.H. Zwietering, I. Jongenburger, F.M. Rombouts, K. van 't Riet, Modeling of the bacterial growth curve, Appl. Environ. Microbiol. 56 (1990) 1875–1881.
[31] Hwai-Shen Liu, Hsien-Wen Hsu, Analysis of gas stripping during ethanol fermentation—I. In a continuous stirred tank reactor, Chem. Eng. Sci. 45 (5) (1990) 1289–1299.
[32] R. Dierstein, G. Drews, Nitrogen-limited continuous culture of Rhodopseudomonas capsulata growing photosynthetically or heterotrophically under low oxygen tensions, Arch. Microbiol. 99 (1) (Jan 1974) 117–128.
[33] E. Boran, E. Özgür, M. Yücel, U. Gündüz, I. Eroglu, Biohydrogen production by Rhodobacter capsulatus Hup− mutant in pilot solar tubular photobioreactor, Int. J. Hydrogen Energy 37 (21) (Nov 2012) 16437–16445.
[34] D.D. Androga, P.H. Sevinç Koku, M. Yücel, U. Gündüz, I. Eroglu, Optimization of temperature and light intensity for improved photofermentative hydrogen production using Rhodobacter capsulatus DSM 1710, Int. J. Hydrogen Energy 39 (2014) 2472–2480.
[35] P. Mullai, E.R. Rene, K. Sridevi, Biohydrogen production and kinetic modeling using sediment microorganisms of Pichavaram mangroves, India BioMed Res. Int. 2013 (2013) 9, article ID 265618.
[36] C.-C. Chen, C.-Y. Lin, J.-S. Chang, Kinetics of hydrogen production with continuous anaerobic culture utilizing sucrose as the limiting substrate, Appl. Microbiol. Biotechnol. 27 (2001) 56–64.
[37] Y. Mu, G. Wang, H.-Q. Yu, Kinetic modeling of batch hydrogen production process by mixed anaerobic cultures, Biores. Technol. 97 (2006) 1302–1307.
[38] P. Mullai, K. Sridevi, Cell growth and product formation kinetics of biohydrogen production using mixed consortia by batch process, Int. J. Chem. Tech. Res. 6 (2014) 5125–5130. ISSN : 0974-4290.
[39] N. Kumar, P.S. Monga, A.K. Biswas, D. Das, Modeling and simulation of clean fuel production by Enterobacter cloacae IIT-BT 08, Int. J. Hydrogen Energy 25 (2000) 945–952.
[40] Y.-C. Lo, W.-M. Chen, C.-H. Hung, S.-D. Chen, J.-S. Chang, Dark H2 fermentation from sucrose and xylose using H2-producing indigenous bacteria: feasibility and kinetic studies, Water Res. 42 (2008) 827–842.
[41] D.D. Androga, E. Özgür, I. Eroglu, U. Gündüz, M. Yücel, Significance of carbon to nitrogen ratio on the long-term stability of continuous photofermentative hydrogen production, Int. J. Hydrogen Energy 36 (24) (Dec 2011) 15583–15594.
[42] R. Sagnak, F. Kargi, Hydrogen gas production from acid hydrolyzed wheat starch by combined dark and photo-fermentation with periodic feeding, Int. J. Hydrogen Energy 36 (17) (Aug. 2011) 10683–10689.
[43] B. Uyar, M. Gürgan, E. Özgür, U. Gündüz, M. Yücel, I. Eroglu, Hydrogen production by hup− mutant and wild-type strains of Rhodobacter capsulatus from dark fermentation effluent of sugar beet thick juice in batch and continuous photobioreactors, Bioproc. Biosyst. Eng. 38 (10) (Oct. 2015) 1935–1942.
[44] J.S. Kim, K. Ito, H. Takahashi, Production of molecular hydrogen in outdoor batch cultures of Rhodopseudomonas sphaeroides, Agric. Biol. Chem. 46 (4) (1982) 937–941.
[45] X.-Y. Shi, H.-Q. Yu, Continuous production of hydrogen from mixed volatile fatty acids with Rhodopseudomonas capsulata, Int. J. Hydrogen Energy 31 (12) (Sep. 2006) 1641–1647.
[46] P. Carlozzi, The effect of irradiance growing on hydrogen photoevolution and on the kinetic growth in Rhodopseudomonas palustris, strain 42OL, Int. J. Hydrogen Energy 34 (19) (Oct. 2009) 7949–7958.
[47] R. Zagrodnik, M. Łaniecki, Hydrogen production from starch by co-culture of Clostridium acetobutylicum and Rhodobacter sphaeroides in one step hybrid dark- and photofermentation in repeated fed-batch reactor, Bioresour. Technol. 224 (Jan. 2017) 298–306.
[48] T. Laurinavichene, K. Laurinavichius, E. Shastik, A. Tsygankov, Long-term H2 photoproduction from starch by co-culture of Clostridium butyricum and Rhodobacter sphaeroides in a repeated batch process, Biotechnol. Lett. 40 (2) (Feb. 2018) 309–314.
[49] E. Özkan, B. Uyar, E. Özgür, M. Yücel, I. Eroglu, U. Gündüz, Photofermentative hydrogen production using dark fermentation effluent of sugar beet thick juice in outdoor conditions, Int. J. Hydrogen Energy 37 (2) (Jan. 2012) 2044–2049.
[50] S.G. Avcioglu, E. Ozgur, I. Eroglu, M. Yucel, U. Gunduz, Biohydrogen production in an outdoor panel photobioreactor on dark fermentation effluent of molasses, Int. J. Hydrogen Energy 36 (17) (Aug. 2011) 11360–11368.
[51] D.D. Androga, E. Ozgur, U. Gunduz, M. Yucel, I. Eroglu, Factors affecting the longterm stability of biomass and hydrogen productivity in outdoor photofermentation, Int. J. Hydrogen Energy 36 (17) (Aug. 2011) 11369–11378.
[52] J. Gebicki, M. Modigell, M. Schumacher, J. van der Burg, E. Roebroeck, Comparison of two reactor concepts for anoxygenic H2 production by Rhodobacter capsulatus, J. Clean. Prod. 18 (Dec. 2010) S36–S42.